

Modulation of LTP/LTD balance in STDP by activity-dependent feedback mechanism

Shigeru Kubota^{a,b,*}, Jonathan Rubin^b, and Tatsuo Kitajima^c

*^aDepartment of Biomedical Information Engineering, Yamagata University,
4-3-16 Jonan, Yonezawa, Yamagata, 992-8510, Japan*

*^bDepartment of Mathematics, University of Pittsburgh,
301 Thackeray Hall, Pittsburgh, PA 15260, USA*

*^cDepartment of Bio-System Engineering, Yamagata University,
4-3-16 Jonan, Yonezawa, Yamagata, 992-8510, Japan*

*Corresponding author. tel: +81-238-26-3738, fax: +81-238-26-3299,

E-mail: kubota@yz.yamagata-u.ac.jp

Abstract

Spike-timing-dependent plasticity (STDP) has been suggested to play a role in the development of functional neuronal connections. However, for STDP to contribute to the synaptic organization, its learning curve should satisfy a requirement that the magnitude of long-term potentiation (LTP) is approximately the same as that of long-term depression (LTD). Without such balance between LTP and LTD, all the synapses are potentiated toward the upper limit or depressed toward the lower limit. Therefore, in this study, we explore the mechanisms by which the LTP/LTD balance in STDP can be modulated adequately. We examine a plasticity model that incorporates an activity-dependent feedback (ADFB) mechanism, wherein LTP induction is suppressed by higher postsynaptic activity. In this model, strengthening an ADFB function gradually decreases the temporal average of the ratio of the magnitude of LTP to that of LTD, whereas enhancing background inhibition augments this ratio. Additionally, correlated inputs can be strengthened or weakened depending on whether the correlation time is shorter or longer than a threshold value, respectively, suggesting that STDP may lead to either Hebbian or anti-Hebbian plasticity outcomes. At an intermediate range of correlation times, the reversal between the two distinct plasticity regimes can occur by changing the level of ADFB modulation and inhibition, providing a physiological mechanism for neurons to select from functionally different forms of learning rules.

Keywords. Plasticity; STDP; Synaptic competition; Cortex; Activity-dependent feedback

1. Introduction

Activity-dependent modification of synaptic transmission, including long-term potentiation (LTP) and long-term depression (LTD), has been widely thought to underlie learning and memory (Bi & Poo, 2001). Although there are various forms of plasticity, recent experiments have revealed that the induction of both LTP and LTD can depend on the relative timing of pre- and postsynaptic spikes (Bi & Poo, 1998; Feldman, 2000; Froemke et al. 2005; Abbott & Nelson, 2000; Caporale & Dan, 2008). In the spike-timing-dependent plasticity (STDP) observed in the neocortical cells, LTP is induced when the presynaptic spike occurs before the postsynaptic spike, while the reversed spike order elicits LTD (Feldman, 2000; Froemke et al. 2005).

STDP learning rule has been suggested to solve a fundamental problem of unbounded synaptic strengthening in Hebbian learning (Song et al., 2000; Song & Abbott, 2001). Hebbian rule of plasticity contributes to the formation of functional circuits and has been used in many neural network studies (Bienenstock et al., 1982; Miller et al., 1989; von der Malsburg, 1973). However, this plasticity rule predicts that when presynaptic inputs are strengthened, the resulting increased postsynaptic activity further strengthens the inputs. Such positive feedback will lead to unlimited growth of synapses, producing instability in the learning dynamics (Miller, 1996). An advantage of STDP is that it can automatically introduce competitive interaction among inputs to stabilize the postsynaptic activity, while maintaining the basic properties of the Hebbian learning (Abbott & Nelson, 2000; Song et al., 2000). Such competition arises from STDP because the inputs that contribute to rapidly evoking the postsynaptic spikes are potentiated, while the others that do not contribute to it are depressed. However, to achieve such competitive function, the magnitude of LTP and LTD in the STDP learning curve should be approximately balanced (Song et al., 2000). When LTP dominates over LTD, all the synapses are potentiated. Conversely, if LTD dominates over LTP, all the synapses are depressed. The fact that synaptic modification dynamics is quite sensitive to the change in the balance between LTP and LTD (Song et al., 2000) may suggest that STDP should be accompanied by an additional mechanism that controls this balance within an adequate range.

Therefore, in this study, we construct a simplified cortical pyramidal neuron model and examine the possible mechanism by which the balance between LTP

and LTD in the STDP learning rule can be regulated. Based on the evidence that LTP in STDP depends on postsynaptic NMDARs (Bender et al., 2006; Egger et al., 1999; Nevian & Sakmann, 2006), which desensitize via the activity-dependent elevation of intracellular Ca^{2+} (Legendre et al., 1993; Medina et al., 1999; Rosenmund et al., 1995), we examine an STDP model, wherein the magnitude of LTP is dynamically modified by such activity-dependent feedback (ADFB) mechanism (Tegnér & Kepecs, 2002; Kubota & Kitajima, 2009). We show that in this model, the temporal average of the LTP/LTD ratio can be gradually increased or decreased by enhancing the background inhibition or strengthening the feedback function, respectively. In addition, we demonstrate that in the presence of the ADFB function, but not in the absence, input correlations function to potentiate or depress a group of correlated inputs depending on the time scale of the input correlation. Furthermore, in an intermediate range of correlation time, the modulation of the strength of ADFB as well as of inhibition can regulate whether the correlated inputs become strengthened or weakened by STDP, providing neurons with the ability to govern the direction of the input correlation-based plasticity.

2. Methods

2.1. Neuron Model

We used a conductance-based pyramidal neuron model consisting of two compartments representing a soma and a dendrite (Kubota & Kitajima, submitted). Both the somatic and dendritic compartments contain voltage-dependent Na^+/K^+ currents (I_{Na} and I_K). A voltage-gated Ca^{2+} current (I_{Ca}) and a Ca^{2+} -dependent potassium current (I_{AHP}) are incorporated into the dendrite to reproduce spike frequency adaptation found in pyramidal cells (Ahmed et al., 1998). The amplitude as well as the kinetic parameters for the voltage-gated currents and I_{AHP} have been adjusted such that the model neuron exhibits instantaneous and adapted f-I curves similar to those of neocortical pyramidal cells (Kubota & Kitajima, submitted).

2.2. Synaptic Currents

The dendritic compartment receives 4000 excitatory and 800 inhibitory synapses, each of which follows the conductance-based model given by Kubota and Kitajima (2008) (Fig. 1A). The level of inhibitory inputs is assumed to depend on a parameter g_{inh} , which represents the peak conductance of GABA-mediated synaptic currents (Kubota & Kitajima, 2008). All the synapses are activated by Poisson processes. The use of Poisson inputs is based on the experimental finding that the spike trains of *in vivo* cortical cells is highly irregular (Softky & Koch, 1993). Excitatory synapses are activated by either uncorrelated spike trains or two groups of spike trains consisting of correlated and uncorrelated ones, while inhibitory synapses are activated by uncorrelated spike trains. All the uncorrelated inputs were generated using independent Poisson spike trains of 3Hz. Taking into account a relatively lower success rate of synaptic transmission in central synapses (~10%) (Hessler et al., 1993), this input rate corresponds to a presynaptic firing rate of ~30 Hz, which is in the physiologically plausible range for the sensory-evoked responses of cortical neurons. In cases where the input correlation is considered (Figs. 5 and 6), excitatory synapses are assumed to consist of two equally sized groups (2000 for each group) and one group of synapses is activated by correlated spike trains, while the other group is activated by uncorrelated spike trains (Song & Abbott, 2001). The presynaptic firing rates for the correlated inputs are generated to have a correlation function that decays exponentially with a time

constant τ_c (correlation time) (Song et al., 2000; Song & Abbott, 2001). The mean (temporally-averaged) firing rate for the correlated inputs is the same as that for the uncorrelated inputs (3 Hz).

2.3. Synaptic Weight Modification by STDP

STDP is assumed to act on all the excitatory synapses. We denote by $\Delta t = t_{post} - t_{pre}$ the time lag between the pre- and postsynaptic events; positive numbers of Δt imply that the presynaptic event preceded the postsynaptic event. The change in the synaptic weight Δw is described as follows (Song et al., 2000) (Fig. 1B):

$$\Delta w = \begin{cases} A_+ \exp(-\Delta t / \tau_+), & \text{for } \Delta t > 0, \\ -A_- \exp(\Delta t / \tau_-), & \text{for } \Delta t < 0, \end{cases} \quad (1)$$

where $A_+ (> 0)$ and $A_- (= 0.004)$ determine the magnitude of synaptic potentiation and depression, respectively, and $\tau_+ = \tau_- = 20$ ms determines the temporal range over which synaptic strengthening and weakening occur. When a pre- or postsynaptic event occurs, the synaptic weights w are modified stepwise by an additive updating rule of STDP. The effects of all the pre- and postsynaptic spike pairs are linearly summed. Upper and lower bounds (w_{max} and 0, respectively) are imposed on each synaptic weight to stabilize learning dynamics.

2.4. Activity-Dependent Modulation of LTP

Recent experiments examining STDP (Bender et al., 2006; Egger et al., 1999; Nevian & Sakmann, 2006) have revealed that LTP and LTD involve distinct signaling pathways that may act as coincidence detectors of pre- and postsynaptic events: the activation of postsynaptic NMDA receptors (NMDARs) for LTP and that of metabotropic glutamate receptors (mGluRs) for LTD. Further, NMDARs have been shown to exhibit intracellular Ca^{2+} -dependent desensitization (Legendre et al., 1993; Medina et al., 1999; Rosenmund et al., 1995), suggesting that LTP, but not LTD, will be suppressed by sustained postsynaptic activity level that results in the accumulation of intracellular Ca^{2+} (Helmchen et al., 1996; Svoboda et al., 1997). Therefore, we consider an activity-dependent feedback (ADFB) of plasticity such that increased postsynaptic activity decreases the magnitude of LTP: $A_+(t) = A_+^0 - kf_{post}(t)$, where $f_{post}(t)$ is the postsynaptic firing rate at time

t ; A_+^0 is the magnitude of LTP when the postsynaptic neuron is almost quiescent (i.e., $f_{post} = 0$); and k (/Hz) is a positive parameter (see below).

Additionally, a line of evidence suggests that the strength of Ca^{2+} -dependent desensitization of NMDARs may be controlled in cortical neurons. Functional NMDARs are composed of NR1 and NR2 (NR2A–NR2D) subunits in the fore-brain (Stephenson, 2001). NR2B-containing NMDARs are predominantly expressed in neonatal neurons, whereas the number of NR2A-containing NMDARs increases over postnatal development (Quinlan et al., 1999a, 1999b). Since the NR2A- but not NR2B-containing NMDARs exhibit Ca^{2+} -dependent desensitization (Krupp et al., 1996), the desensitization can be expected to be facilitated through the NMDAR subunit switch. Moreover, the expression pattern of distinct NR2 subunits is modulated depending on the neuronal activity or the neurotrophin level (Quinlan et al., 1999a, 1999b; Caldeira et al., 2007), implying that NMDAR subunit composition can change across different conditions. Therefore, to incorporate the effects of changes in NMDAR subunit expression into our model, we define a non-dimensional parameter ρ ($0 \leq \rho \leq 1$) such that $\rho = 0$ denotes the state where the NR2B subunits are predominant, as in the case of very immature neurons, whereas $\rho = 1$ represents the state where the NR2A subunits are fully expressed, as in mature neurons. Then, if we denote by k_{\max} the maximum value of the feedback gain parameter k provided by the NR2A-containing NMDARs, the ADFB modulation of the magnitude of LTP (Fig. 1B) can be described as

$$A_+(t) = A_+^0 - k_{\max} \rho f_{post}(t). \quad (2)$$

Here, the postsynaptic firing rate at each time point was calculated by $f_{post}(t) = \int_0^\infty \lambda \exp(-\lambda \tau) S_{post}(t - \tau) d\tau$, with the output spike train represented by $S_{post}(t) = \sum_{t_{post}} \delta(t - t_{post})$ and $\lambda = 0.1$ /s (Tanabe & Pakdaman, 2001). The parameter values used in the ADFB function itself are $A_+^0 = 0.008$ and $k_{\max} = 0.068$ ms.

3. Results

3.1. Impact of LTP/LTD Balance on Learning Dynamics by STDP

To investigate how the LTP/LTD balance in the STDP curve affects learning dynamics, we examined the equilibrium properties of STDP (i.e., the state where the synaptic weights converge to a stationary distribution) for various values of the LTP size A_+ without ADFB (i.e., $\rho = 0$). In Fig. 2, we plotted the average weight (Fig. 2A) and the mean firing rate of the neuron (Figs. 2B and 2C) as function of the A_+/A_- ratio for three different values of inhibitory conductance g_{inh} . The figure shows that the equilibrium state of STDP changes abruptly over a small range of A_+/A_- (Song et al., 2000; Rubin et al., 2001): if A_+/A_- is slightly greater than 1, the synaptic weights are increased toward the upper limit so that the postsynaptic firing rate becomes much higher. Conversely, if A_+/A_- becomes less than 0.98, the synapses are strongly depressed and, therefore, the postsynaptic activity becomes much lower. On the other hand, the increased level of inhibition (larger g_{inh}) can gradually decrease the postsynaptic activity for all values of A_+/A_- (Figs. 2B and 2C). The finding that the neuronal activity is drastically changed in a very narrow range of A_+/A_- (Fig. 2C) implies that to regulate neuronal activity adequately, the LTP/LTD ratio should also be precisely controlled.

To explore the possibility that the ADFB mechanism (Eq. 2) regulates the LTP/LTD ratio, we simply take the temporal average of Eq. 2 to obtain the following relationship:

$$\overline{A_+/A_-(t)} = A_+^0/A_- - \alpha \overline{f_{post}(t)}, \quad (3)$$

with $\alpha = k_{max}\rho/A_-$. Here, $\overline{x(t)} = T^{-1} \int_t^{t+T} x(t')dt'$ ($T \gg 1$) represents the temporally averaged value of $x(t)$. Therefore, $\overline{A_+/A_-(t)}$ is the temporal mean of the LTP/LTD ratio and $\overline{f_{post}(t)}$ is the mean firing rate of the postsynaptic neuron. The relationship between $\overline{A_+/A_-(t)}$ and $\overline{f_{post}(t)}$ in Eq. 3 was plotted, for given values of ρ , as shown in Figs. 2B and 2C (thin lines). If the temporal fluctuation of A_+/A_- is not so large, it might be expected that the values of $\overline{A_+/A_-(t)}$ and $\overline{f_{post}(t)}$ obtained by STDP, in the presence of ADFB modulation,

would correspond to the intersection point between 2 different curves—the line representing Eq. 3 for a given ρ (thin lines) and the postsynaptic rate vs. A_+/A_- curve (thick lines) for a given g_{inh} —in Fig. 2B.

Note that the increase in the strength of ADFB modulation (larger ρ) will move the intersection point such that the value of A_+/A_- at this point becomes slightly decreased, as can be seen from Fig. 2B. This implies the possibility that by changing the parameter ρ , the mean value of the A_+/A_- ratio at the equilibrium of STDP might be gradually modified within a very small range of $A_+/A_- \sim 1$. Moreover, Fig. 2B also indicates that the enhanced inhibition (larger g_{inh}) would shift the position of the intersection point so that the A_+/A_- ratio becomes slightly increased. Therefore, in the following section, we examine how the changes in the strength of the ADFB mechanism, as well as the background inhibition level, can regulate the LTP/LTD balance in the STDP curve and thereby influence the learning dynamics.

3.2. Control of the LTP/LTD Balance through ADFB and Inhibitory Mechanisms

To explore the role of the ADFB function and inhibition in controlling the LTP/LTD balance, we investigated the equilibrium properties of STDP in the presence of ADFB modulation for various values of ρ and g_{inh} . Since the random synaptic activation, as well as the temporal variation in the synaptic distribution, produces fluctuation in the firing activity, the time course of the A_+/A_- ratio is irregular even at the equilibrium (Fig. 3). However, as the ADFB modulation is facilitated by increasing ρ , the temporally averaged value of the A_+/A_- ratio was found to converge to a value slightly smaller than 1 (Figs. 4A and 4B), as predicted in Fig. 2B (Tegnér & Kepecs, 2002). In the presence of this approximate balance in LTP and LTD, a small reduction in the A_+/A_- ratio considerably decreases the average weight as well as the postsynaptic firing rate (Figs. 4C and 4D) (Song et al., 2000). Therefore, the strengthening of ADFB by a further increase in ρ is counterbalanced by the weakening of the postsynaptic activity, and the temporal average of A_+/A_- decreases very gradually with increasing ρ (Fig. 4B) (Kubota & Kitajima, submitted).

On the other hand, changing g_{inh} does not significantly affect the postsynaptic firing rate for larger ρ ($\rho > 0.4$) (Fig. 4D). Instead, stronger inhibition augments the average weight via a small increase in the LTP/LTD ratio (Figs. 4B and 4C). This finding suggests that our model exhibits a strong regulatory function that maintains the excitatory-inhibitory balance through the precise control of the LTP/LTD balance. Furthermore, the coefficient of variation (CV) for the interspike intervals (ISIs) in the output spike train was found to increase with ρ and g_{inh} in the range of larger ρ values (Fig. 4E). The higher ISI variability caused by the enhanced inhibition is attributable to the fact that larger g_{inh} increases the average synaptic weight (Fig. 4C). This effect reduces the number of excitatory inputs needed to reach the threshold voltage and prevent the temporal integration of inputs from producing regular firing pattern (Softky & Koch, 1993). Although larger ρ acts to weaken the synapses (Fig. 4C), this effect will be overcome by decreasing the postsynaptic firing rate (Fig. 4D); since, at lower firing rates, the effective passive decay for the membrane voltage is increased, the neuron will behave as a coincidence detector and thereby can produce an irregular firing pattern (Liu & Wang, 2001).

Additionally, as shown in Figs. 4B and 4D (open symbols), we plotted the values of A_+/A_- and the postsynaptic firing rate corresponding to the intersection points shown in Fig. 2B (see Sec. 3.1), which were calculated by performing the linear interpolation of the firing rate vs. A_+/A_- relationship for each g_{inh} (thick lines in Fig. 2B). Figures 4B and 4D indicate that the results obtained by the numerical simulation with the ADFB mechanism (closed symbols) show very good agreement with those predicted by this intersection argument (open symbols).

3.3. ADFB modulation in the presence of correlated inputs

The above results suggest that ADFB may provide STDP with a strong regulatory function such that the postsynaptic firing rate is kept almost constant for a given value of ρ (Fig. 4D). To examine how such regulatory action affects learning dynamics in the presence of correlated inputs, we divided synapses into two equally-sized groups and introduced correlation into one of them (Song & Abbott, 2001; see Methods). The other group remained uncorrelated so that we could compare the effects of ADFB on the correlated and uncorrelated inputs.

Physiological experiments examining correlated neuronal activity suggest that the time scale of correlation ranges widely from milliseconds to seconds (Mastrojarde, 1983; Bach & Kruger, 1986; Brivanlou et al., 1998; Lampl et al., 1999; Bair et al., 2001; Reich et al., 2001; Kohn & Smith, 2005); the sharing of the same afferent inputs produces correlated spiking on a millisecond time scale (Mastrojarde, 1983), whereas the temporal variation in firing activity caused by changing sensory stimuli can generate correlation on a time scale of seconds (Bair et al., 2001; Bach & Kruger, 1986). Therefore, we performed simulations by using a wide range of correlation time τ_c ($5 \text{ ms} < \tau_c < 5 \text{ s}$), the results of which are presented in Figs. 5A–5C. Here, to clarify the impact of ADFB, the results of both using and not using ADFB (left and right column, respectively) are shown. The value of A_+/A_- for the case without ADFB ($A_+/A_- = 0.975$) was chosen such that the steady-state weight distribution becomes approximately the same for the two models with smaller τ_c ($\tau_c = 10 \text{ ms}$; Fig. 5A). As shown in the figure, with such smaller correlation time, the correlated synapses gather near either the upper or lower boundary, whereas the uncorrelated synapses are depressed toward the lower boundary (Song and Abbott, 2001). However, as the correlation time is increased, all the synapses are pushed toward the lower limit in the absence of ADFB (Fig. 5B, right), converging to a unimodal distribution, whereas in the presence of ADFB, the correlated and uncorrelated inputs tend to decrease and increase, respectively, converging to a bimodal distribution (Fig. 5B, left). Therefore, in the presence, but not absence of ADFB, there is a threshold value of τ_c such that the correlated inputs are strengthened or weakened, compared to the uncorrelated inputs, depending on whether the value of τ_c is smaller or larger than the threshold, respectively (Figs. 5C and 5D).

It should be noted that a group of inputs having longer correlation time cannot quit firing after evoking postsynaptic spikes, increasing the number of post-pre timing spike pair that induces LTD (Song et al., 2000). Therefore, it is not surprising that, in both the presence and absence of ADFB, the synaptic strength of correlated inputs was decreased by increasing τ_c (Fig. 5C). An interesting feature of ADFB is that it can function to compensate for the decline of the correlated inputs by increasing the LTP/LTD ratio (Fig. 5E). This in turn strengthens the uncorrelated inputs (Fig. 5C, left), since their synaptic drift is primarily determined by the

integral of the STDP curve (Song and Abbott, 2001; Rubin et al., 2001). Thus, the increase in the uncorrelated inputs can counterbalance the decrease in the correlated inputs to maintain the postsynaptic activity (Fig. 5F). This will also be understood from Fig. 2B; the thin lines in this figure, which represents the relationship of Eq. 3, show that ADFB keeps the postsynaptic firing rate at an almost constant value as long as LTP and LTD are approximately balanced.

To further explore the input correlation-based synaptic modifications under the effects of ADFB, we performed similar calculations while changing the strengths of ADFB modulation and of inhibition (Fig. 6). The correlation time dependence of the strength of the correlated and uncorrelated inputs (Figs. 6A and 6B) and the difference between them (Fig. 6C) as well as the LTP/LTD ratio (Fig. 6D) was found to be strongly modified by alterations in ρ and g_{inh} . Figures 6A and 6B suggest that the synaptic strength of either/both group(s) tends to accumulate very close to the upper or lower limit for a range of very small or large values of τ_c , so that the separation of the two groups of weights becomes saturated under the influence of the boundaries (Fig. 6C). The LTP/LTD ratio is increased and decreased, in a wide range of τ_c , by smaller ρ and g_{inh} , respectively (Fig. 6D), which is consistent with the previous results for uncorrelated input cases (Fig. 4B). Additionally, it can be found that in a particular range of τ_c ($80 \text{ ms} < \tau_c < 400 \text{ ms}$), the correlated inputs can be either strengthened or weakened, compared to uncorrelated inputs, depending on the values of ρ and g_{inh} (Fig. 6C). This effect implies that the changes in ρ and g_{inh} could regulate which among correlated and uncorrelated inputs become strengthened by STDP. This was clarified by performing the same simulations while systematically changing the values of ρ and g_{inh} in the case of $\tau_c = 160 \text{ ms}$, as shown in Fig. 6E. The figure demonstrates that changes in these physiological parameters can modulate both the direction and the magnitude of the input correlation-dependent synaptic modifications emerging from STDP.

4. Discussion

In this study, we have examined an STDP model incorporating an ADFB mechanism, wherein higher postsynaptic activity decreases the magnitude of LTP so that the LTP/LTD ratio is modified dynamically. When a postsynaptic neuron receives random uncorrelated inputs, the temporal average of the LTP/LTD ratio (A_+ / A_-) in the STDP curve was increased and decreased gradually, within a range slightly smaller than 1, by increasing g_{inh} and ρ , respectively (Figs. 2B and 4B). The strengths of ADFB and inhibition therefore provide physiological mechanisms by which the LTP/LTD balance in STDP can be precisely controlled. Importantly, for a given value of ρ , changing g_{inh} does not significantly change the postsynaptic firing activity (Fig. 4D). This finding suggests that ADFB achieves a strong regulatory function that maintains the level of neuronal activity by slightly modulating the LTP/LTD ratio (Figs. 4B and 4D). We further studied the cases where the input consists of two groups of synapses, where one group is correlated and the other group is uncorrelated. In this case, as the correlation time (τ_c) is prolonged, the dominant group was switched under ADFB modulation such that the correlated and uncorrelated groups become dominant for smaller and longer τ_c , respectively (Figs. 5C (left) and 5D). This switch in the direction of input correlation-based plasticity represents an additional regulatory function emerging from ADFB. When the prolonged correlation weakens the correlated synapses (Fig. 5C (left); Song & Abbott, 2001), ADFB can produce a bias in the LTP/LTD ratio toward LTP (Fig. 5E) and counterbalance the decrease in the correlated synapses by the increase in the uncorrelated ones, keeping the neuronal activity nearly constant (Fig. 5F). Interestingly, the direction of the input correlation-based plasticity can reverse with changes in the values of ρ and g_{inh} , within a certain intermediate range of τ_c (Fig. 6E), providing a possible mechanism for tuning a system's response properties in response to stimulus characteristics.

4.1. Physiological mechanisms regulating LTP/LTD balance in STDP

The synaptic dynamics resulting from STDP has been shown to have an important advantage of being competitive, unlike the rate-based models of Hebbian plasticity (Song et al., 2000). However, the induction of such a competitive function critically depends on an approximate balance in LTP and LTD in the STDP curve

(Song et al., 2000; Rubin et al., 2001). Considering the fact that such LTP/LTD balance is generally not found in the learning curves obtained by experiments using pairing protocols (e.g., Bi & Poo, 1998), it appears likely that an additional mechanism may be involved in regulating this balance in biological systems.

The present results have shown that the ADFB mechanism can maintain an approximate balance in LTP and LTD (Fig. 4B); moreover, modulation of the strength of ADFB as well as of inhibition, provided by the activation of GABA conductance, has been found to be effective in very gradually modulating this balance. As mentioned above, a line of evidence suggests that the magnitude of ADFB can be altered under physiological conditions; first, the induction of LTP, but not LTD, depends on the activation of postsynaptic NMDARs (Bender et al., 2006; Egger et al., 1999; Nevian & Sakmann, 2006), indicating that the LTP/LTD ratio depends on the activity level of NMDARs. Second, the Ca^{2+} -dependent desensitization of NMDARs will be found in NR2A- but not NR2B-containing NMDARs (Krupp et al., 1996), suggesting that switching from NR2B to NR2A subunits will promote the activity-dependent desensitization of NMDARs mediated by the Ca^{2+} influx through voltage-dependent Ca^{2+} channels (Medina et al., 1999). Therefore, we consider that the coordination between NMDAR subunit expression and GABA conductance may be involved in the control of the LTP/LTD balance in the STDP learning rule.

Importantly, the primary role of the ADFB mechanism in our model is to prevent the saturation of synaptic weights so that the firing rate is maintained in a reasonable range (Fig. 2). Therefore, it would be possible to regulate the LTP/LTD balance by using more general mechanisms that can maintain the firing activity in the neuronal circuits, such as homeostatic plasticity (Turrigiano & Nelson, 2004). Additionally, since the physiological mechanisms that control the expression pattern of distinct NMDAR subunits (Caldeira et al., 2007) or provide subunit-specific modulation of NMDAR-mediated synaptic currents (Yuen et al., 2005) will be expected to alter the strength of ADFB modulation, it appears likely that these mechanisms can contribute to regulating the LTP/LTD balance in biological systems. It has also been shown that the LTP/LTD balance can be precisely regulated, similar to the present study, by using the STDP model involving synaptic modification based on a biophysical Ca^{2+} -dependent plasticity model (Kubota & Kitajima, submitted).

4.2. Hebbian and anti-Hebbian plasticity in STDP

The notion of Hebbian plasticity has guided much work in both experimental and theoretical neuroscience (Buonomano & Merzenich, 1998; Feldman & Brecht, 2005). At a level of cortical organization, a Hebbian-based learning rule contributes to detecting correlated inputs and expanding the representation of such inputs. This would be effective to augment the cortical processing capacity of behaviorally relevant inputs, given that the peripheral inputs that fire at similar times are likely to represent points that are close together on peripheral sensory units (Buonomano & Merzenich, 1998).

STDP has been considered important as a mechanism for realizing Hebbian-based plasticity in natural conditions (Abbott, 2003). STDP can strengthen a group of correlated inputs and promote the organization of neuronal connections in an activity-dependent manner (Song & Abbott, 2001). The present study has revealed that when STDP is accompanied by the ADFB mechanism, it can strengthen or weaken the correlated inputs as compared to uncorrelated ones when the correlation time is shorter or longer than a threshold, respectively (Fig. 5D). This result suggests that STDP can act as either a Hebbian or an anti-Hebbian learning rule depending on the correlation structure of afferent inputs. Furthermore, this finding is reminiscent of recent observations of barrel map plasticity (Polley et al., 2004; Polley et al., 1999; Feldman & Brecht, 2005), which have revealed that transferring rats from home cages to a natural environment induces the contraction of the representation of frequently-used whiskers as well as the sharpening of the whisker map. Based on our results, we can predict that the contraction of frequently-activated inputs may occur through the appearance of prolonged correlation times within the firing activity of the neuronal subpopulation representing the inputs to the barrel cortex (Fig. 5D). Since the time scale of the correlations will significantly depend on that of changing input stimuli (Bach & Kruger, 1986; Simons, 1978), it appears conceivable that the observed change in barrel map plasticity (Polley et al., 2004; Polley et al., 1999) may result from the alteration in the time course of whisker movement caused by active exploration of a natural environment.

Another source of correlated firing arises through synchronized membrane fluctuations, which consist of ‘up’ and ‘down’ states, and is frequently observed

between nearby cortical neurons (Lampl et al., 1999; Anderson et al., 2000; Kohn & Smith, 2005; Castro-Alamancos, 2009). The correlation of the two-state membrane potential fluctuation is stronger in pairs of cortical neurons that respond to the same aspects of sensory stimuli (Lampl et al., 1999), and additionally, this type of correlated firing is enhanced by the stimulus presentation (Anderson et al., 2000), suggesting that it plays a role in the stimulus-dependent cortical processing. For a range of correlation time (80–400 ms), nearly corresponding to the time scale of correlation by the membrane potential fluctuation (Lampl, et al., 1999; Anderson et al., 2000; Castro-Alamancos, 2009), our model predicts that whether the correlated inputs are potentiated or depressed depends on the level of ADFB and GABA inhibition (Fig. 6E). Therefore, the combination of the cortical membrane fluctuation and the ADFB modification of STDP may provide the neurons with the ability to select from Hebbian or anti-Hebbian rule such that the inputs arising from sensory stimuli can be strengthened or weakened compared to those from the background spontaneous activity. The cortical network may use Hebbian plasticity to increase the response to the behaviorally important stimuli by strengthening the connections from such stimuli to widely distributed neurons. On the other hand, anti-Hebbian plasticity may be beneficial when animals are in an environment containing many stimuli so that a more efficient method for representing each sensory stimulus is required (Polley et al. 2004). Therefore, we consider that the proposed mechanism for selecting from functionally distinct forms of plasticity rules may be useful to permit efficient distribution of limited metabolic resources for achieving cortical representation of stimuli.

Acknowledgements

This study is partially supported by the Grant-in-Aid for Scientific Research (KAKENHI (19700281), Young Scientists (B)) from the Japanese government. S.K. is partially supported by the Program to Accelerate the Internationalization of University Education from the Japanese government and the International Research Training Program from Yamagata University. J.R. is partially supported by the U.S. National Science Foundation Award DMS 0716936.

References

- Abbott, L. F. (2003). Balancing homeostasis and learning in neural circuits. *Zoology*, *106*, 365–371.
- Abbott, L. F., & Nelson, S. B. (2000). Synaptic plasticity: taming the beast. *Nature Neuroscience*, *3*(Suppl), 1178–1183.
- Ahmed, B., Anderson, J. C., Douglas, R. J., Martin, K. A. C., & Whitteridge, D. (1998). Estimates of the net excitatory currents evoked by visual stimulation of identified neurons in cat visual cortex. *Cerebral Cortex*, *8*, 462–476.
- Anderson, J., Lampl, I., Reichova, I., Carandini, M., & Ferster, D. (2000). Stimulus dependence of two-state fluctuations of membrane potential in cat visual cortex. *Nature Neuroscience*, *3*, 617–621.
- Bach, M., & Kruger, J. (1986). Correlated neuronal variability in monkey visual cortex revealed by a multi-microelectrode. *Experimental Brain Research*, *61*, 451–456.
- Bair, W., Zohary, E., & Newsome, W. T. (2001). Correlated firing in macaque visual area MT: Time scales and relationship to behavior. *Journal of Neuroscience*, *21*, 1676–1697.
- Bender, V. A., Bender, K. J., Brasier, D. J., & Feldman, D. E. (2006). Two coincidence detectors for spike timing-dependent plasticity in somatosensory cortex. *Journal of Neuroscience*, *26*, 4166–4177.
- Bi, G. Q., & Poo, M. M. (1998). Synaptic modifications in cultured hippocampal neurons: Dependence on spike timing, synaptic strength, and postsynaptic cell type. *Journal of Neuroscience*, *18*, 10464–10472.
- Bi, G. Q., & Poo, M. M. (2001). Synaptic modification by correlated activity: Hebb's postulate revisited. *Annual Review of Neurosciences*, *24*, 139–166.
- Bienenstock, E. L., Cooper, L. N., & Munro, P. W. (1982). Theory for the development of neuron selectivity: Orientation specificity and binocular interaction in visual cortex. *Journal of Neuroscience*, *2*, 32–48.
- Brivanlou, I. H., Warland, D. K., & Meister, M. (1998). Mechanisms of concerted firing among retinal ganglion cells. *Neuron*, *20*, 527–539.
- Buonomano, D. V., & Merzenich, M. M. (1998). Cortical plasticity: From synapses to maps. *Annual Reviews of Neuroscience*, *21*, 149–86.
- Caldeira, M. V., Melo, C. V., Pereira, D. B., Carvalho, R. F., Carvalho, A. L., & Duarte, C. B. (2007). BDNF regulates the expression and traffic of NMDA re-

- ceptors in cultured hippocampal neurons. *Molecular and Cellular Neuroscience*, 35, 208–219.
- Caporale, N., & Dan, Y. (2008). Spike timing-dependent plasticity: A Hebbian learning rule. *Annual Review of Neurosciences*, 31, 25–46.
- Castro-Alamancos, M. A. (2009, in press). Cortical up and activated state: Implications for sensory information processing. *Neuroscientist*.
- Egger, V., Feldmeyer, D., & Sakmann, B. (1999). Coincidence detection and change of synaptic efficacy in spiny stellate neurons in rat barrel cortex. *Nature Neuroscience*, 2, 1098–1105.
- Feldman, D. E. (2000). Timing-based LTP and LTD at vertical inputs to layer II/III pyramidal cells in rat barrel cortex. *Neuron*, 27, 45–56.
- Feldman, D. E., & Brecht, M. (2005). Map plasticity in somatosensory cortex. *Science*, 310, 810–815.
- Froemke, R. C., Poo, M. M., & Dan, Y. (2005). Spike-timing-dependent synaptic plasticity depends on dendritic location. *Nature*, 434, 221–225.
- Helmchen, F., Imoto, K., & Sakmann, B. (1996). Ca^{2+} buffering and action potential-evoked Ca^{2+} signaling in dendrites of pyramidal neurons. *Biophysical Journal*, 70, 1069–1081.
- Hessler, N. A., Shirke, A. M., & Mallnow, R. (1993). The probability of transmitter release at a mammalian central synapse. *Nature*, 366, 569–572.
- Kohn, A., & Smith, M. A. (2005). Stimulus dependence of neuronal correlation in primary visual cortex of the macaque. *Journal of Neuroscience*, 25, 3661–3673.
- Krupp, J. J., Vissel, B., Heinemann, S. F., & Westbrook, G. L. (1996). Calcium-dependent inactivation of recombinant N-methyl-d-aspartate receptors is NR2 subunit specific. *Molecular Pharmacology*, 50, 1680–1688.
- Kubota, S., & Kitajima, T. (2008). A model for synaptic development regulated by NMDA receptor subunit expression. *Journal of Computational Neuroscience*, 24, 1–20.
- Kubota, S., & Kitajima, T. (2009, in press). How balance between LTP and LTD can be controlled in spike-timing-dependent learning rule. *In Proceedings of the 2009 international joint conference on neural networks (IJCNN 2009)*.
- Kubota, S., & Kitajima, T. (submitted). Possible role of cooperative action of NMDA receptor and GABA function in developmental plasticity.

- Lampl, I., Reichova, I., & Ferster, D. (1999). Synchronous membrane potential fluctuations in neurons of the cat visual cortex. *Neuron*, *22*, 361–374.
- Legendre, P., Rosenmund, C., & Westbrook, G. L. (1993). Inactivation of NMDA channels in cultured hippocampal neurons by intracellular calcium. *Journal of Neuroscience*, *13*, 674–684.
- Liu, Y. H., & Wang, X. J. (2001). Spike-frequency adaptation of a generalized leaky integrate-and-fire model neuron. *Journal of Computational Neuroscience*, *10*, 25–45.
- Mastrorarde, D. N. (1983). Correlated firing of cat retinal ganglion cells. I. Spontaneously active inputs to X- and Y-cells. *Journal of Neurophysiology*, *49*, 303–324.
- Medina, I., Leinekugel, X., & Ben-Ari Y. (1999). Calcium-dependent inactivation of the monosynaptic NMDA EPSCs in rat hippocampal neurons in culture. *European Journal of Neuroscience*, *11*, 2422–2430.
- Miller, K. D. (1996). Synaptic economics: Competition and cooperation in synaptic plasticity. *Neuron*, *17*, 371–374.
- Miller, K. D., Keller, J. B., & Stryker, M. P. (1989). Ocular dominance column development: Analysis and simulation. *Science*, *245*, 605–615.
- Nevian, T., & Sakmann, B. (2006). Spine Ca^{2+} signaling in spike-timing-dependent plasticity. *Journal of Neuroscience*, *26*, 11001–11013.
- Polley, D. B., Chen-Bee, C. H., & Frostig, R. D. (1999). Two directions of plasticity in sensory-deprived adult cortex. *Neuron*, *24*, 623–637.
- Polley, D. B., Kvasnak, E., & Frostig, R. D. (2004). Naturalistic experience transforms sensory maps in the adult cortex of caged animals. *Nature*, *429*, 67–71.
- Quinlan, E. M., Olstein, D. H., & Bear, M. F. (1999a). Bidirectional, experience-dependent regulation of N-methyl-d-aspartate receptor subunit composition in the rat visual cortex during postnatal development. *Proceedings of the National Academy of Sciences of the United States of America*, *96*, 12876–12880.
- Quinlan, E. M., Philpot, B. D., Hugarir, R. L., & Bear, M. F. (1999b). Rapid, experience-dependent expression of synaptic NMDA receptors in visual cortex in vivo. *Nature Neuroscience* *2*, 352–357.
- Reich, S., Mechler, F., & Victor, J. D. (2001). Independent and redundant information in nearby cortical neurons. *Science*, *294*, 2566–2568.

- Rosenmund, C., Feltz, A., & Westbrook, G. L. (1995). Calcium-dependent inactivation of synaptic NMDA receptors in hippocampal neurons. *Journal of Neurophysiology*, *73*, 427–430.
- Rubin, J., Lee, D. D., & Sompolinsky, H. (2001). Equilibrium properties of temporally asymmetric Hebbian plasticity. *Physical Review Letters*, *86*, 364–367.
- Simons, D. J. (1978). Response properties of vibrissa units in rat SI somatosensory neocortex. *Journal of Neurophysiology*, *41*, 798–820.
- Softky, W. R., & Koch, C. (1993). The highly irregular firing of cortical cells is inconsistent with temporal integration of random EPSPs. *Journal of Neuroscience*, *13*, 334–350.
- Song, S., & Abbott, L. F. (2001). Cortical development and remapping through spike timing-dependent plasticity. *Neuron*, *32*, 339–350.
- Song, S., Miller, K. D., & Abbott, L. F. (2000). Competitive Hebbian learning through spike-timing-dependent synaptic plasticity. *Nature Neuroscience*, *3*, 919–926.
- Stephenson, F. A. (2001). Subunit characterization of NMDA receptors. *Current Drug Targets*, *2*, 233–239.
- Svoboda, K., Denk, W., Kleinfeld, D., & Tank, D. W. (1997). In vivo dendritic calcium dynamics in neocortical pyramidal neurons. *Nature*, *385*, 161–165.
- Tanabe, S., & Pakdaman, K. (2001). Noise-enhanced neuronal reliability. *Physical Review E*, *64*, 041904.
- Tegnér, J., & Kepecs, Á. (2002). Why neuronal dynamics should control synaptic learning rules. *Advances in Neural Information Processing Systems*, *14*, 285–292.
- Turrigiano, G. G., & Nelson, S. B. (2004). Homeostatic plasticity in the developing nervous system. *Nature Reviews Neuroscience* *5*, 97–107.
- von der Malsburg, C. (1973). Self-organization of orientation selective cells in the striate cortex. *Kybernetik*, *14*, 85–100.
- Yuen, E. Y., Jiang, Q., Chen, P., Gu, Z., Feng, J., & Yan, Z. (2005). Serotonin 5-HT_{1A} receptors regulate NMDA receptor channels through a microtubule-dependent mechanism. *Journal of Neuroscience*, *25*, 5488–5501.

Figure legends

Figure 1. Components of the computational model. (A) A postsynaptic neuron receives Poisson inputs from both excitatory and inhibitory synapses. The excitatory inputs are plastic and their strength is modified by STDP. (B) The magnitude of LTP in the STDP learning curve is dynamically modulated by feedback depending on postsynaptic firing rate (f_{post}) (Eqs. 1 and 2).

Figure 2. Predicted effects of changing the LTP/LTD ratio (A_+ / A_-) on the equilibrium properties of STDP. Thick lines: The values of average weight (A) and the mean firing rate (B and C), obtained by STDP without ADFB (i.e., $\rho = 0$), were plotted as function of A_+ / A_- , for three different values of the inhibitory conductance g_{inh} ($g_{inh} = 3.75, 5, \text{ or } 6.25 \mu\text{S}/\text{cm}^2$). Note that different ranges of A_+ / A_- are used in (B) and (C). Thin lines in (B) and (C): The linear relationship between $\overline{A_+ / A_-}(t)$ and $\overline{f_{post}}(t)$ specified by Eq. 3 for $\rho = 0.6$ and 0.8 .

Figure 3. The time course of the A_+ / A_- ratio at the equilibrium state of STDP ($\rho = 0.5$ and $g_{inh} = 6.25 \mu\text{S}/\text{cm}^2$).

Figure 4. The equilibrium properties of the STDP model incorporating an ADFB mechanism. The temporally averaged values of the A_+ / A_- ratio (A and B) and the average weight over all the synapses (C), the mean postsynaptic firing rate (D), and the CV for the ISIs (E) are plotted as function of ρ for three different values of g_{inh} ($g_{inh} = 3.75, 5, \text{ or } 6.25 \mu\text{S}/\text{cm}^2$). (B) shows the higher magnification of the A_+ / A_- ratio in (A). Open symbols in (B) and (D): The values of A_+ / A_- and the postsynaptic firing rate obtained by the intersection points in Fig. 2B (see Sec. 3.1). The difference in the firing rates for the three cases of g_{inh} is invisible in the open symbols in (D).

Figure 5. The equilibrium properties of the STDP model when the neuron receives both correlated and uncorrelated inputs. (A–C) The steady-state weight distributions (A and B) and the relationship of the average weight vs. the correlation time (C) for the correlated (red) and uncorrelated (black) input groups. The ADFB

modulation is active in the left column, but inactive in the right column. The correlation times used for (A) and (B) are $\tau_c = 10$ and 1280 ms, respectively. (D–F) The difference in the average weight between the correlated and uncorrelated groups (D), the temporal mean of the LTP/LTD ratio (E), and the postsynaptic firing rate (F) are shown as a function of τ_c . The solid and dashed lines show the cases with and without ADFB mechanism, respectively.

Figure 6. The effects of changing the strength of ADFB (ρ) and the inhibition level (g_{inh}) on the equilibrium properties of STDP in the presence of both correlated and uncorrelated groups of inputs. (A and B) The average weights for the correlated (red) and uncorrelated (black) groups at the equilibrium of STDP are plotted as function of the correlation time τ_c . In (A), the impact of changing ρ is examined, where $\rho = 0.8$ (solid) or 0.6 (dashed). In (B), the impact of changing g_{inh} is examined, where $g_{inh} = 5$ (thick line) or 3.75 $\mu\text{S}/\text{cm}^2$ (thin line). ($g_{inh} = 5 \mu\text{S}/\text{cm}^2$ in (A) and $\rho = 0.8$ in (B)) (C and D) The difference in the average weights between the correlated and uncorrelated groups (C) and the temporally averaged value of A_+ / A_- (D) are plotted by using the same line types as those in (A) and (B). ($(\rho, g_{inh}) = (0.8, 5)$ (thick solid), $(0.6, 5)$ (dashed), or $(0.8, 3.75)$ (thin solid)) (E) The difference in the average weight between the two input groups as a function of ρ and g_{inh} , where $\tau_c = 160$ ms. The correlated inputs are potentiated or depressed, as compared to the uncorrelated inputs, depending on the values of ρ and g_{inh} .

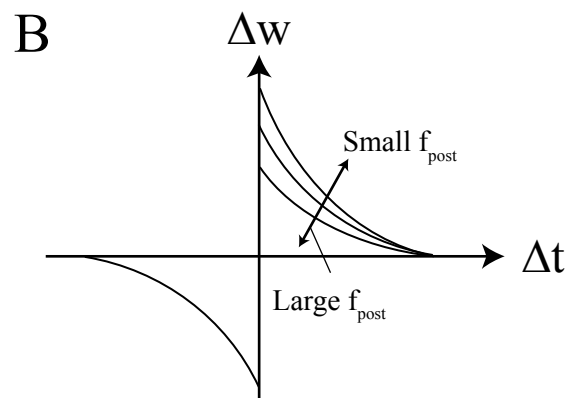
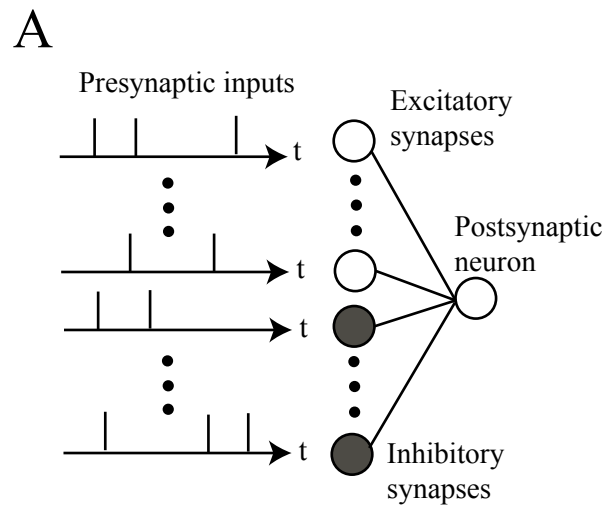


Figure 1. Kubota et al.

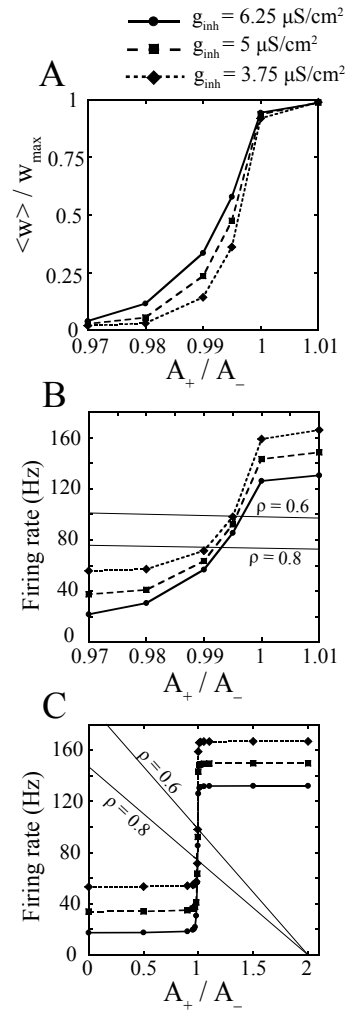


Figure 2. Kubota et al.

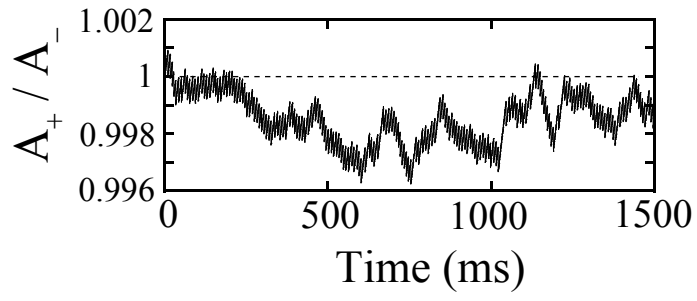


Figure 3. Kubota et al.

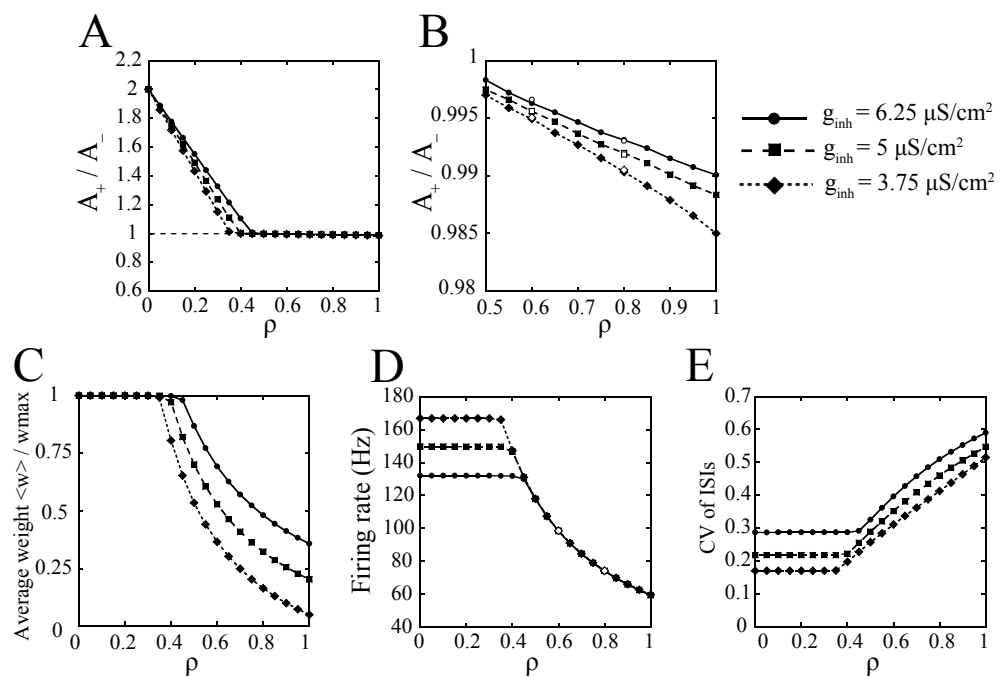


Figure 4. Kubota et al.

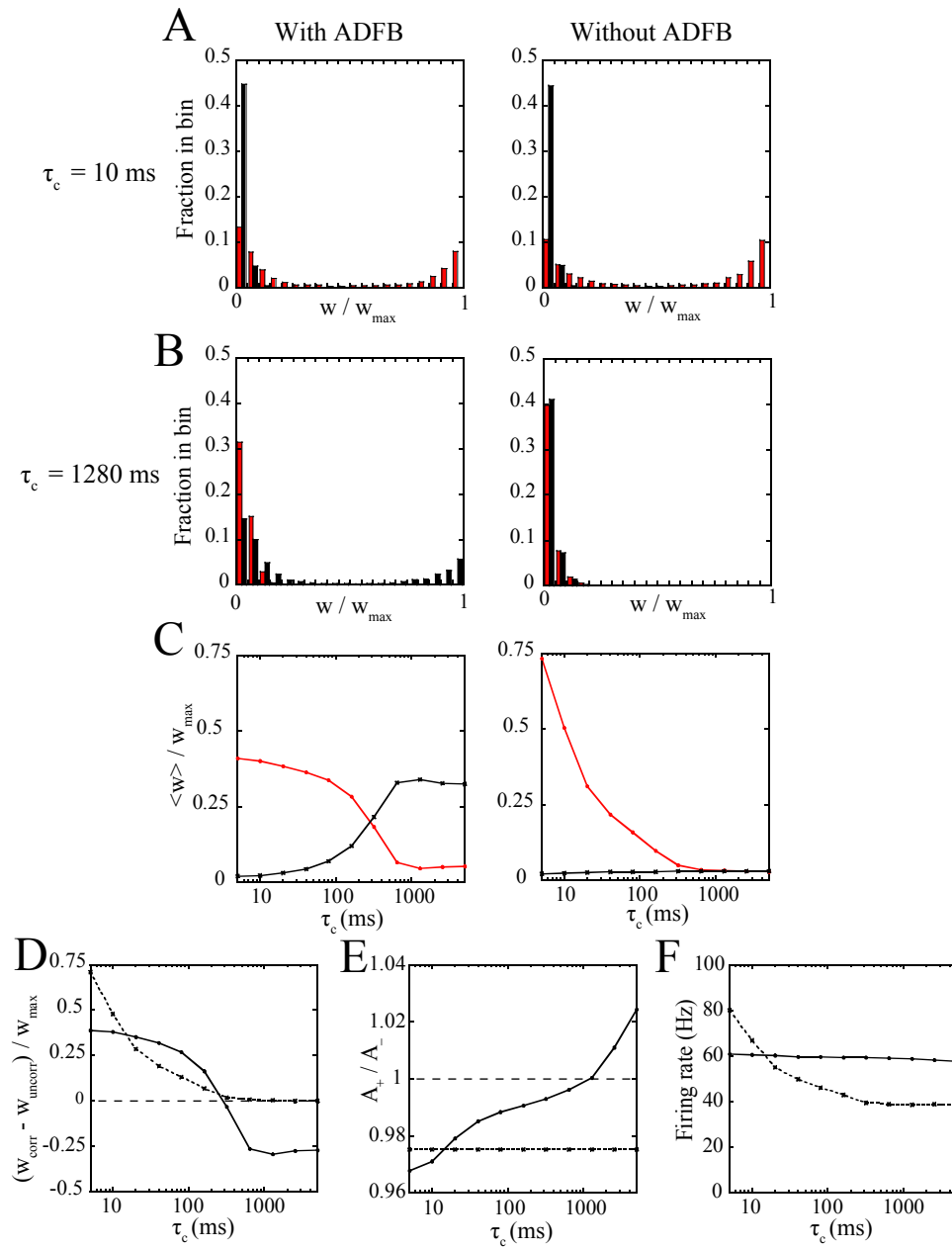


Figure 5. Kubota et al.

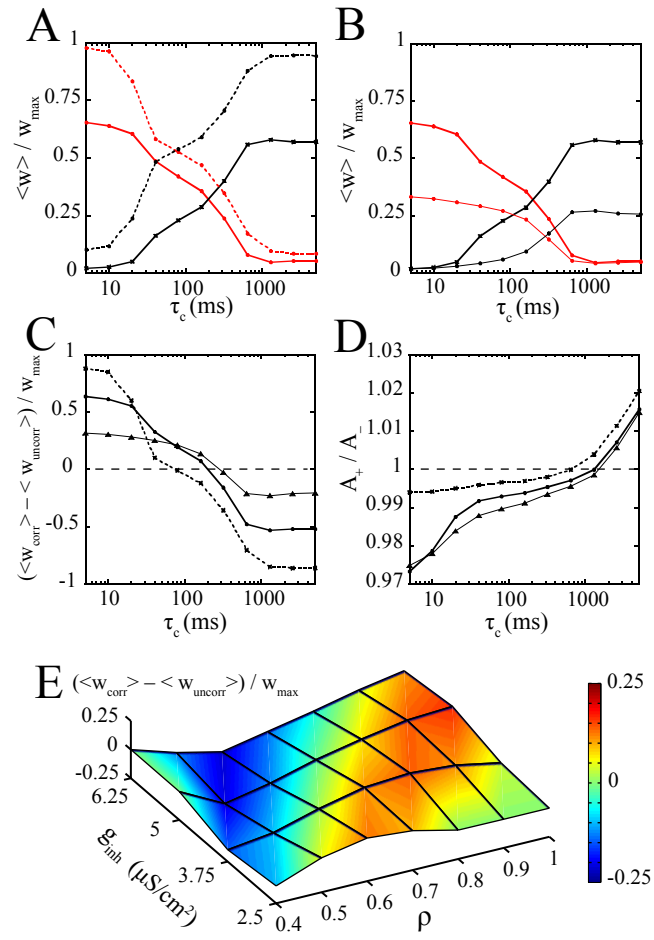


Figure 6. Kubota et al.